# AB Statens Anläggningsprovning

Alströmergatan 12 · Box 49306 · 100 28 STOCKHOLM · Tel. 08–54 10 20

# DYNAMIC ANALYSIS OF CRACK GROWTH AND ARREST IN A PRESSURE VESSEL SUBJECTED TO THERMAL AND PRESSURE LOADING

BJÖRN BRICKSTAD, SA
FRED NILSSON, SKI

SA/FoU-RAPPORT 84/06
(SKI-projekt nr B32/84).

# DYNAMIC ANALYSIS OF CRACK GROWTH AND ARREST IN A PRESSURE VESSEL SUBJECTED TO THERMAL AND PRESSURE LOADING

Björn Brickstad
The Swedish Plant Inspectorate, Box 49306, 100 28 Stockholm, Sweden

Fred Nilsson*
Swedish Nuclear Power Inspectorate, Box 27106, 102 52 Stockholm, Sweden

Abstract

Predictions of crack arrest behaviour are performed for a cracked reactor pressure vessel under both thermal and pressure loading. The object is to compare static and dynamic calculations. The dynamic calculations are made using an explicit finite element technique where crack growth is simulated by gradual nodal release. Three different load cases and the effect of different velocity dependence on the crack propagation toughness are studied. It is found that for the analysed cases the static analysis is slightly conservative, thus justifying its use for these problems.

* Author to receive all correspondance about the paper.

## Introduction

In order to investigate whether a crack growth event ends in crack arrest a dynamic analysis must in general be performed. Such an analysis is in most cases quite cumbersome and a fully dynamic treatment of crack propagation under three-dimensional conditions requires unrealistic computing times on computers available today. Therefore quasi-static methods are almost exclusively used in engineering analyses of crack propagation and arrest events. It is obviously of interest to investigate the relevance and accuracy of quasi-statically performed predictions.

The nuclear energy field is probably the one where the most efforts on the problem of crack arrest have been spent. In recent years the possible consequences of a pressurized thermal shock (PTS) have been analysed with respect to crack arrest and this has greatly stimulated the interest in the subject. By a pressurized thermal shock is there meant that a sudden cooling of a reactor pressure vessel occurs while it is pressurized or that a re-pressurization takes place during a cooling transient. In older reactor vessels embrittlement because of neutron irradiation may have occured and in some cases undercladding defects are present. Therefore the severe stressing during a pressurized thermal shock is a potential cause of rapid crack growth. In order to investigate this complicated and costly experiments (Bryan et al [1] ) have recently been performed. Cheverton et al [2] performed dynamic and static FEM-calculations of thermal shock events and found that the static method may be either conservative or unconservative depending on the exact conditions. However, the deviations between the results from the two methods were fairly small. Jung and Kanninen [3] have made similar calculations of a ther-

mal shock experiment and found the quasi-statically computed results to be slightly unconservative. These results indicate that for situations of the type considered it may not be necessary to perform dynamic calculations.

It should be immediately realized that the last statement can not have general validity. It is therefore necessary to perform comparative analyses of a number of cases in order to find the conditions under which a quasi-static treatment can be safely used.

In the present investigation such a comparative analysis is performed for loading cases that may occur in the vessel of a pressurized water reactor (PWR) if a major pipe should break. The analysis is performed within the linear elastic theory of dynamic crack growth and under the assumption of two-dimensional (plane strain) conditions.

## Basic assumptions

A two-dimensional body under plane strain mode I conditions contains a crack. The crack tip position is measured by the variable a. The initiation and growth laws are under linear elasto-dynamic conditions assumed to be of the following form.

A crack will not start to grow from rest if (1) is satisfied.

$$K_I^d < K_{Ic}(T) \qquad (1)$$

$K_I^d$ is the dynamically calculated stress-intensity factor and $K_{Ic}$ is the fracture toughness which in general depends on the temperature T at the position of the tip.

During growth eqn. (2) holds.

$$K_I^d = K_{pc}\ (T,\ \dot{a}) \qquad (2)$$

$K_{pc}$ is a material function depending on crack tip velocity and temperature. Finally, the crack will come to a momentary stop if (3) is fulfilled.

$$K_I^d < K_{pc}\ (T,\ \dot{a}=0) = K_{Ia}\ (T) \qquad (3)$$

$K_{Ia}$ is here termed the crack arrest toughness and is not necessarily equal to $K_{Ic}$. Even if the crack tip comes to rest according to (3) the crack growth may be reinitiated if dynamic effects cause $K_I^d$ to reach above $K_{Ic}$.

To which extent the linear theory outlined is relevant has not yet been investigated to a satisfactory degree of understanding. A discussion on the subject of non-linear effects on crack growth can be found in a recent paper by Nilsson and Brickstad [4]. These complications will however be ignored in the present article.

Since $K_I^d$ depends on the entire history and not only on the instantaneous conditions a fully dynamic analysis must in general be performed. In <u>quasi-static</u> treatment $K_I^d$ is replaced by the statically calculated stress-intensity factor $K_I^s$. Since $K_I^s$ only depends on the momentary conditions, the arrest length $a^*$ is given directly as the solution of eqn. (4).

$$K_I^s\ (a^*) = K_{Ia}\ (T(a^*)) \qquad (4)$$

In this case the previous history does not enter the arrest condition and the computational effort is greatly reduced.

Numerical technique

The numerical analysis involves the solution of a time dependent boundary value problem consisting of a crack moving through the reactor pressure vessel, subjected to arbitrary mechanical and/or thermal loading. Here, a very long axial edge-crack is assumed to exist on the inner surface of the vessel so that the problem can be analysed under two-dimensional plane strain conditions. The FEM-model of a cross section is shown in fig. 1. The geometry is taken from a typical pressurized water reactor.

Due to symmetry, only half a ring of the vessel needs to be modelled giving a total of 655 quadrilateral and triangular elements and a minimum of 1454 degrees of freedom for zero crack length. The inner layer corresponds to a 4 mm thick cladding with the intention of in future investigation studying the effect of different material behaviour of the cladding as compared to the base material.

An elastodynamic FEM-program was developed, using an explicit method based on the central difference approximation to integrate the equations of motion. The crack growth model adopted here is the by now rather well established gradual nodal relaxation technique, introduced by Rydholm et al [5]. In the FEM-mesh a closing force $F_c$ is introduced at the nearest node behind the current position of the crack tip. The magnitude of $F_c$ depends on the crack-tip position $\delta(t)$ within the finite element distance d as

$$F_c = F_o \, (1 - \delta(t)/d)^{1/2} \qquad (5)$$

Here $F_o$ is the force in this node immediately before the relaxation begins. $F_o$ is thus gradually relaxed to zero as the crack propagates through the element length d. $\delta(t)$ is a known function of time if the crack velocity å is known. The dynamic energy release rate G is then obtained by calculating the work performed by $F_c$ over the distance d, and thus the dynamic stress intensity factor can be determined from the wellknown relation between $K_I^d$ and G.

A simulation of a typical crack propagation and arrest event was performed in the following way.

First the initial static state is determined for the particular loading and the chosen initial crack length. It is then assumed that $K_{Ic}(T)$ coincides with $K_I^s$ so that growth starts. With the static solution as input into the dynamic analysis the crack is growing with a velocity å, for each finite element along the crack plane, corresponding to a root to eqn. (6).

$$f(å) = K_I^d - K_{pc}(T, å) = 0 \qquad (6)$$

Assuming $K_{pc}$ to be known, the particular crack velocity å for which f=0 is determined with a simple iterative technique, described by Brickstad and Nilsson [6]. If crack arrest occurs, the solution of (6) gives å=0 for a certain crack length a*. Since no energy is consumed for a stationary crack the nodal release method cannot be used for calculation of $K_I^d$ after a crack arrest. Instead, a technique denoted as a calibrated nodal displacement method, first introduced by Walsh [7], was used to calculate $K_I^d$. It utilizes the relation between $K_I^d$ and the time dependent crack opening displacements (COD). Due to numerical errors from the FEM-mesh, the COD are then calibrated

by comparing the static K evaluated from COD with standard solutions. The correction was here of the order of 10 per cent.
If (1) is not satisfied at all times succeeding a crack arrest, reinitiation of the crack growth is possible.

## Description of studied examples

As a model for the study a typical pressurized water reactor of the three-loop type was chosen. As mentioned above the vessel is assumed to have a very long axial edge-crack. This is of course a very conservative assumption compared to a realistic case.
The mechanical data of the material are those of A508B and are given in table 1. For the sake of simplicity the cladding material is assumed to have the same mechanical properties and thermal expansion coefficient as A508B in the FEM-calculations. Judging by the results of Nied [8], this should not influence the crack arrest lengths very much. However, in the calculation of the temperature distribution the different thermal properties of the cladding were considered. These and the thermal properties of A508B are also given in table 1.
Two different temperature distributions were considered and are shown in fig. 2. The curve marked SLB is the temperature 200 seconds after a steam-line break as reported for the considered reactor by Evans [9]. The temperature was here computed by a straight forward one-dimensional finite difference code. Similarly the curve marked LOCA represents the temperature 200 seconds after a complete break of one coolant pipe in the hot leg. It should be pointed out that this particular time instant does not give the most severe loadings. It was, however, chosen for the following reason. The rather unrealistic assumption of an

infinitely long crack makes crack arrest impossible once the crack growth is initiated for the more severe loading cases. The object of this study was mainly to study if crack arrest really occurs when the quasi-static treatment predicts this and thus the milder loading cases were considered.

The pressure load 200 seconds after a steamline break is according to [9] 6.55 MPa. Together with the temperature curve SLB this combined loading is termed loading case A. A second loading case B was defined as the temperature curve SLB together with a pressure of 14.5 MPa in order to study the effect of different proportions between thermal and pressure loading. The third loading case C is simply the LOCA temperature curve and thus no pressure load. In fig. 3 the hoop stress distribution due to the different loading cases is shown.

The fracture properties used in this study are the relations derived in [1] and by Pugh [10] based on observations on PTS.

$$K_{Ic} = 51.276+51.897 \exp(0.036(T-RT_{NDT})) \text{ MPa}\sqrt{m} \quad (7)$$

$$K_{Ia} = 35.0+33.279 \exp(0.02408(T-RT_{NDT})) \text{ MPa}\sqrt{m} \quad (8)$$

Both $K_{Ic}$ and $K_{Ia}$ are bounded by the commonly assumed shelf-level of 220 MPa$\sqrt{m}$.

$RT_{NDT}$ is here the nil-ductility temperature of the material in $^{o}C$. The $K_{pc}$-relation was taken from [10].

$$K_{pc} = K_{Ia} + A\,\hat{a}^2 \quad (9)$$

$$A = \begin{cases} [32.97+1.625(T-RT_{NDT})]\cdot 10^{-5} \text{ MPam}^{-3/2}\text{s}^2, & T-RT_{NDT} \geq 0 \\ 32.97\ 10^{-5} \text{ MPam}^{-3/2}\text{s}^2 & T-RT_{NDT} < 0 \end{cases} \quad (10)$$

The conditional choice of the parameter A in eqn. (10) is introduced to avoid a negative slope in the $K_{pc}$-å relation, which is in conflict with most experimental observations and furthermore causes difficulties in the numerical treatment. Eqns. (9) and (10) give the temperature - and velocity dependence on $K_{pc}$ and is shown in fig. 4. It turned out that for the actual velocities encountered in the computer runs, the velocity effect on $K_{pc}$ was fairly small. Therefore one run was made with A replaced by $A' = 10$ A in order to study the sensitivity of the results to variations of $K_{pc}(å)$.

The $RT_{NDT}$-temperature was chosen so that crack growth initiation occured for the considered initial crack length $a_o$ and the loading case considered. Since the loadings were not very severe this resulted in unrealistically high $RT_{NDT}$-values. In spite of this we believe, however, that the chosen fracture properties are such that the main features of real crack growth-arrest events are retained, at least what regards the difference between a quasistatic and a fully dynamic treatment.

## Results and discussion

A calibration of the FEM-grid used was made by comparing the static stress intensity factor $K_I^s$ calculated from the mesh in fig. 1, with other available solutions. In fig. 5 this comparison is shown for the steam line break, loading case A. The reference solution is taken from Buchalet and Bamford [11] . Here $K_I^s$ is given for a crack in a cylinder wall with the same

ratio of radius to thickness as in this study and with a stress-distribution in form of an arbitrary third-degree polynomial. $K_I^s$ from the present FEM-grid was evaluated by the same energy method as in the dynamic case, i.e. by calculating the static energy release rate when relaxing a nodal force to zero, thereby causing a crack growth. For the static calculations the general finite element program ADINA was used. The agreement in fig. 5 between the two solutions for loading case A is very good. The maximum relative deviation can be estimated to four per cent except perhaps for very short crack lengths. This gives some confidence as to the accuracy that can be expected with the present FEM-mesh.

We now turn to the result of the evaluated crack arrest events for the different loading cases A, B and C. In figs. 6-9 the different stress intensity factors ($K_I^s$,$K_I^d$) and the crack velocity å are shown as functions of the crack length a. As mentioned previously $RT_{NDT}$ is chosen in such a way that the curves of $K_{Ic}(T)$ and $K_{Ia}(T)$ according to eqns. (9) and (10), intersect the curve of $K_I^s(a)$ for certain crack lengths. For the initial crack length $a_o$ corresponding to $K_I^s=K_{Ic}(T(a_o))$, the crack starts to grow with a velocity å determined so that the growth equation (6) is satisfied. A dynamically predicted crack arrest is obtained when $K_I^d=K_{Ia}$. The crack length at which this occurs is to be compared with the quasi-statically predicted arrest length, i.e. the intersection between $K_I^s$ and $K_{Ia}(T(a))$.The symbols in the figures are refering to the midside of the finite elements along the crack plane. A crack arrest is however attributed to a position corresponding to a nodal point in the FEM-grid along the crack plane.

In all cases in figs. 6-9, the same principal behaviour is shown. For short crack lengths there is little difference between $K_I^s$ and $K_I^d$ (fig. 6). As the crack propagates deeper into the pressure vessel, $K_I^d$ increases more slowly than $K_I^s$ for the following reasons. Waves emitted from the crack tip and reflected at the outer boundary will not reach the tip again during the first part of the growth. Therefore $K_I^d$ initially varies as if the crack propagated in a semi-infinite body. As the crack grows further, information about the boundaries gradually reaches the tip and $K_I^d$ falls somewhere between $K_I^s$ and the semi-infinite value.

A crack arrest is then predicted at a shorter crack length than is the case of a quasi-static treatment. Apparently, kinetic energy is radiated from the crack-tip and all is not recovered by reflected waves before a crack arrest has occured.

For loading case A with $RT_{NDT}$=198.6°C, there exists two crack lengths for which $K_I^s(a)=K_{Ic}(T)$. Figs. 6-7 show the arrest events for rapid crack growth starting from both these initial crack lengths. The same dynamically predicted arrest length is obtained for the two cases.

Load case B and C are meant to illuminate the effect of different proportions between thermal and mechanical loading. In load case B a steam line break is considered with the internal pressure raised to 14.5 MPa. It is worth noting (fig. 8) that a crack arrest is here predicted in the dynamic evaluation whereas no crack arrest is predicted with a quasi-static treatment. Also in load case C (LOCA with zero internal pressure), the conservatism in the quasi-static analysis is confirmed (fig. 9), and it does not seem that altering the proportion between primary and secondary loading will change this conclusion.

The case shown in fig. 6 was also run with a modified $K_{pc}$-å relation in that the parameter A in eqn. (9) is replaced by $A'$=10A. The results from this run are shown

in fig. 10 and it is found that $K_I^d$ is almost the same as in fig. 6 while the arrest lengths coincide. The only difference is that the increased velocity dependence gives a considerably lower velocity.

In fig. 11, $K_I^d$ is plotted versus time both before and after the time of crack arrest for the event previously shown in fig. 6. After the arrest has occurred, $K_I^d$ shows an oscillatory behaviour. It should be pointed out that similar oscillations are probably present during the propagation event, but these are averaged out by the evaluation technique. In a real structure where damping is present $K_I^d$ should approach the static stress-intensity factor $K_I^s$ at the arrest length. Since damping is neglected, some overshootings above $K_I^s(a^*)$ are observed. The amplitude of these overshootings are quite small, and the major ones occur after about 2200 μs and 4000 μs after the initiation of the crack growth. This times are approximately the arrivals of the dilatational and shear waves, respectively, after these have been emitted at initiation and traveled around the mean circumference of the vessel.

At the arrest length in fig. 11, $K_{Ic}$=220 MPa$\sqrt{m}$. Therefore, judging from fig. 11, the arrested crack will not reinitiate, at least if dynamic effects have a negligible influence on the initiation value of $K_I$ . This can not be verified for a certainty since $\dot{K}_I^d$, immediately after the crack has been arrested, is of the order of $10^5$-$10^6$ MPa$\sqrt{m}$/s during a short time interval, and this may cause a decrease of $K_{Ic}$.

## Concluding remarks

Some important conclusions can be drawn in view of the presented results. Firstly, if the studied run-arrest events were to reflect actual experimental situations

in order to determine the fracture properties of the material, then a quasi-static treatment would overestimate the arrest toughness $K_{Ia}$. This is consistent with e.g. results from crack arrest experiments on SEN-specimens reported by Brickstad [12]. For other geometries and loading conditions it is possible to obtain the opposite relation. Kalthoff et al [13] found for crack arrest experiments with long crack jumps in DCB-specimens that $K^d_{Ia} < K^s_{Ia}$. Similarly, Cheverton et al [2] found the same behaviour when analysing a hypothetical case which resulted in a large crack jump. Their assumptions were, however, very unrealistic as what regards the $K_{pc}$-å relation in that $K_{pc}$ was assumed constant and equal to 62 MPa$\sqrt{m}$. The conclusion is that in general, and particularly for evaluation of this kind of PTS-problems, dynamic effects should be taken into account in order to establish the crack arrest capability of the material. However, when the dynamic fracture properties are sufficiently well known, predictions of crack growth and arrest will produce conservative results (longer crack arrest lengths) with a quasi-static analysis. Hence, it is suggested that for design purposes, to predict the arrest length for the kind of loaded pressure vessels studied here, a quasi-static treatment is sufficiently conservative, at least if the analysis predicts a limited amount of crack growth. This is an important aspect in view of the complexity and cost involved when performing fully dynamic analyses. The typical running time for the problems considered in this investigation was 5 CPU-hours on a UNIVAC 1100/61 computer. Unfortunately it is not possible to state in any precise terms when there is a risk that a quasi-static treatment is un-conservative. Judging from the present results and those presented in[3]it seems that for engineering purposes the quasi-static method can be used in predictions of PTS-events.

Acknowledgement

This work was sponsored by the Swedish Nuclear Power Inspectorate. We want to express our gratitude for this support. We furthermore want to thank Ms. Martina Nyström and Mr. Leif Pettil for helpful assistance with the preparation of the manuscript.

References

[1] R.H. Bryan, B.R. Bass, S.E. Bolt, J.W. Bryson, J.G. Merkle, G.C. Robinson and G.D. Whitman, Quick-Look report on the first pressurized thermal shock, PTSE-1, Oak Ridge National Laboratory ORNL/PTSE-1, 1984.

[2] R.D. Cheverton, P.C. Gehlen, G.T. Hahn and S.K. Iskander, Application of crack arrest theory to a thermal shock experiment, *Crack Arrest Methodology and Applications*, ASTM STP 711, American Society for Testing and Materials, 392-421, 1980.

[3] J. Jung and M.F. Kanninen, An analysis of dynamic crack propagation and arrest in a nuclear pressure vessel under thermal shock conditions, *J. of Pressure Vessel Tech.*, 105, 111-116, 1983.

[4] F. Nilsson and B. Brickstad, Dynamic fracture mechanics-rapid crack growth in linear and non-linear materials, *Elastic Plastic Fracture Mechanics*, ASFM 4, ISPRA, to appear.

[5] G. Rydholm, B. Fredriksson and F. Nilsson, Numerical investigations of rapid crack propagation, *Numerical Methods in Fracture Mechanics*, University of Swansea, 660-672, 1978.

[6] B. Brickstad and F. Nilsson, Explicit time integration in FEM analysis of dynamic crack propagation, *Numerical Methods in Fracture Mechanics*, University of Swansea, 473-487, 1980.

[7] P.F. Walsh, Stress intensity factors by calibrated finite element method, *J. of the Eng. Mech. Div*, ASCE, 98, 1611-1614, 1972.

[8] H.S. Nied, Thermal shock in a circumferentially cracked hollow cylinder with cladding, Eng. Fract. Mech., 20, 113-137, 1984.

[9] C.I.L. Evans, Fracture mechanics evaluation of the Ringhals 2 reactor vessel, Westinghouse Nuclear International WENX/79/21, 1979.

[10] C.E. Pugh, Preliminary pretest definition of the first wide-plate crack-arrest test to be performed for the heavy-section steel technology program, Oak Ridge National Laboratory, 1984.

[11] C.B. Buchalet and W.H. Bamford, Stress-intensity factor solutions for continous surface flaws in reactor pressure vessels, *Mechanics of Crack Growth*, ASTM STP 590, American Society for Testing and Materials, 385-401, 1976.

[12] B. Brickstad, A FEM analysis of crack arrest experiments, *Int. J. Fract.*, 21, 177-191, 1983.

13 J.F. Kalthoff, J. Beinert, S. Winkler and W Klemm, Experimental analysis of dynamic effects in different crack arrest test specimens, *Crack Arrest Methodology and Applications*, ASTM STP 711, American Society for Testing and Materials, 109-127, 1983.

Figure captions

Fig. 1 Finite element model of the pressure vessel.

Fig. 2 Temperature distribution 200 s after a steam-line break and a loss-of-coolant accident respectively. After [9].

Fig. 3 Hoop stress distribution for the different loading cases.

Fig. 4 Assumed $K_{pc}$ versus å relation for different relative temperatures.

Fig. 5 Comparison of static stress-intensity factors from the present calculations and from [11].

Fig. 6 $K_{Ic}$, $K_{Ia}$, $K_I^s$, $K_I^d$ and å as functions of crack length for SLB with p=6.55 MPa. $a_o$=4 mm.

Fig. 7 $K_{Ic}$, $K_{Ia}$, $K_I^s$, $K_I^d$ and å as functions of crack length for SLB with p=6.55 MPa. $a_o$=32 mm.

Fig. 8 $K_{Ic}$, $K_{Ia}$, $K_I^s$, $K_I^d$ and å as functions of crack length for SLB with p=14.5 MPa. $a_o$=18 mm.

Fig. 9 $K_{Ic}$, $K_{Ia}$, $K_I^s$, $K_I^d$ and å as functions of crack length for LOCA. $a_o$=53 mm.

Fig. 10 $K_{Ic}$, $K_{Ia}$, $K_I^s$, $K_I^d$ and å as functions of crack length for SLB with p=6.55 MPa and modified $K_{pc}$-å relation. $a_o$=4 mm.

Fig. 11 $K_I^d$ as a functions of time for SLB with p=6.55 MPa. $a_o$=4 mm.

Table 1. Mechanical and thermal properties

| | A508B | Cladding |
|---|---|---|
| Young's modulus (MPa) | $1.97 \cdot 10^5$ | - |
| Poisson's ratio | 0.3 | - |
| Conductivity ($W/m^oC$) | 43 | 17 |
| Heat capacity ($J/kg^oC$) | 500 | 488 |
| Thermal expansion coefficient $^oC^{-1}$ | $12.3 \cdot 10^{-6}$ | - |

Fig. 1

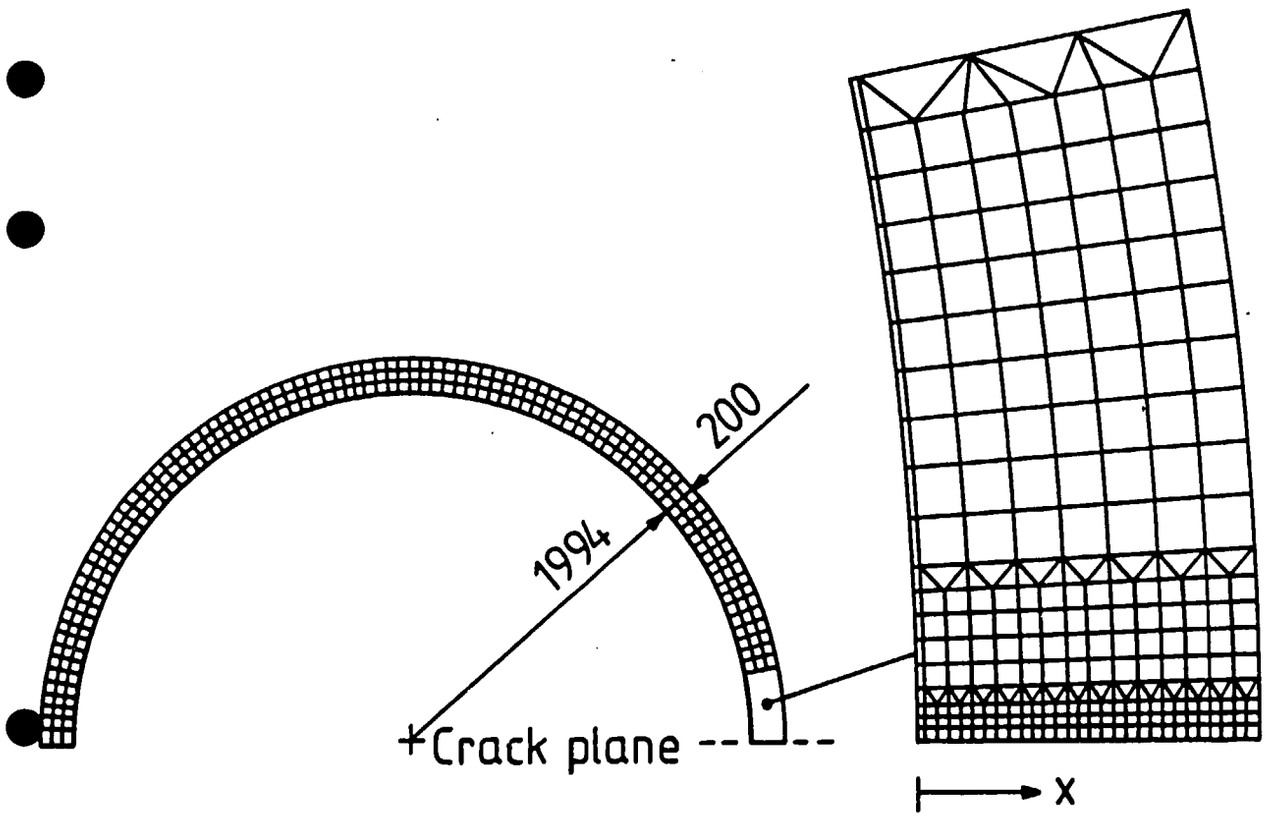

Fig. 2

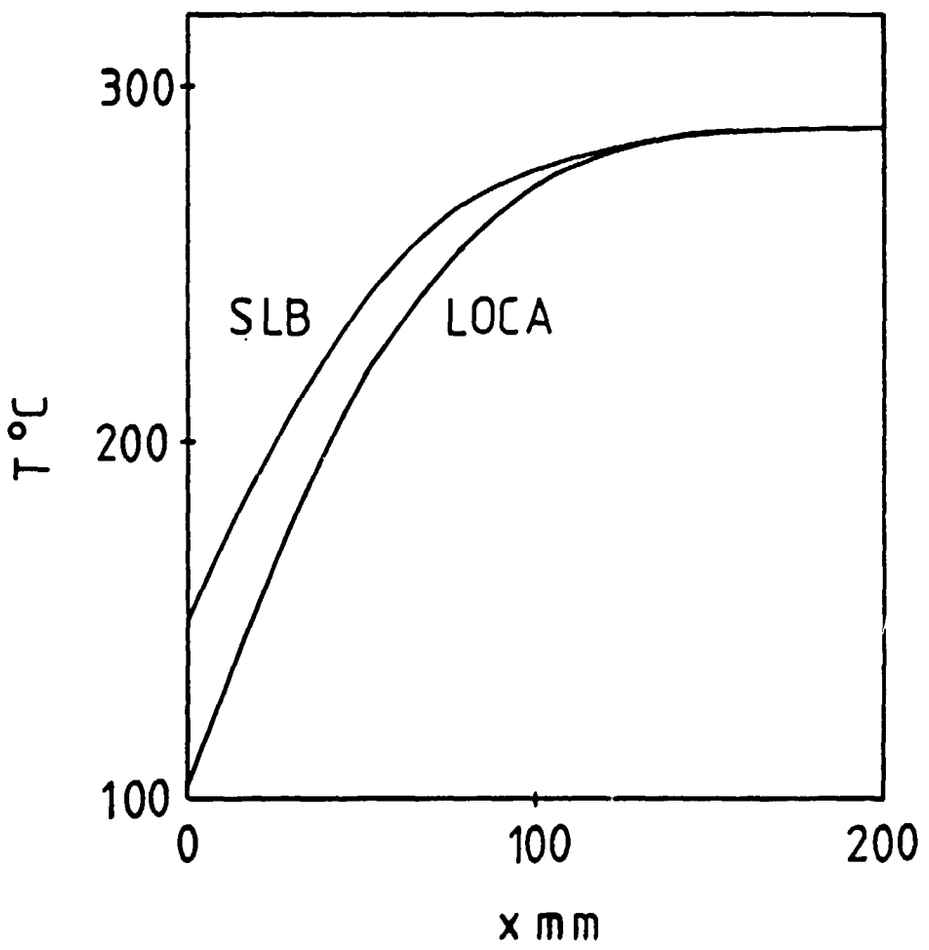

Fig. 3

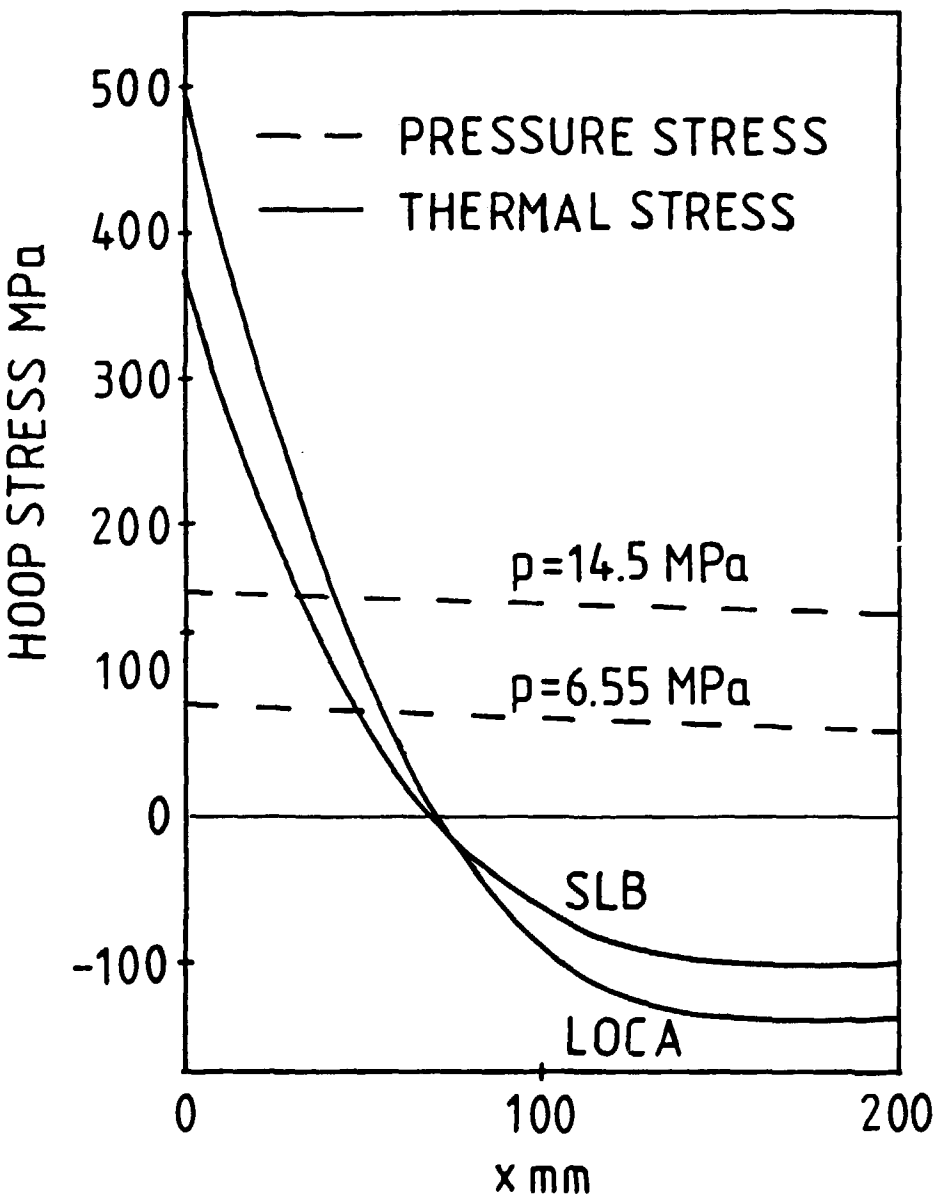
500
400
300
200
100
0
-100
HOOP STRESS MPa
PRESSURE STRESS
THERMAL STRESS
p=14.5 MPa
p=6.55 MPa
SLB
LOCA
0
100
200
x mm

Fig. 4

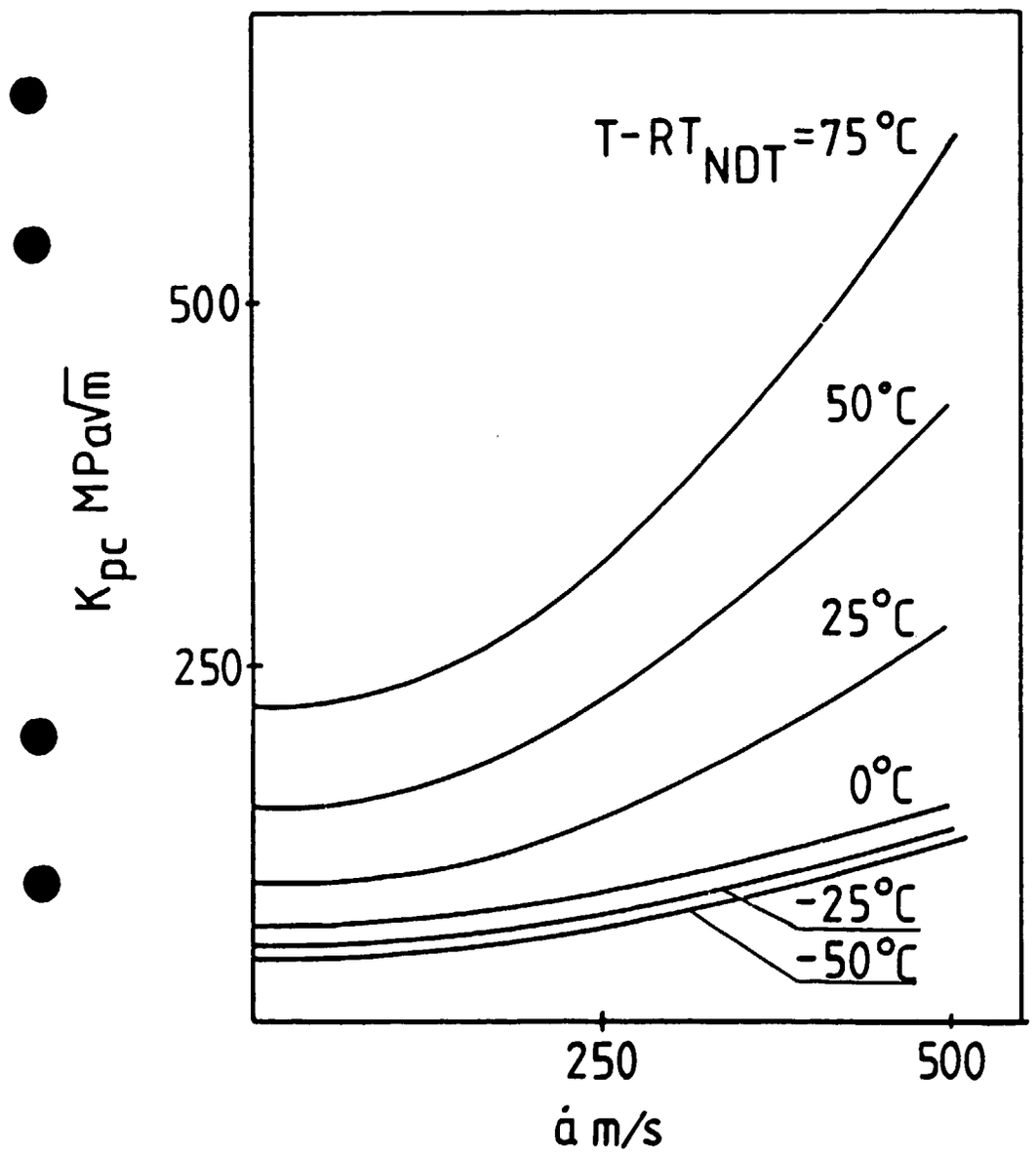

Fig. 5

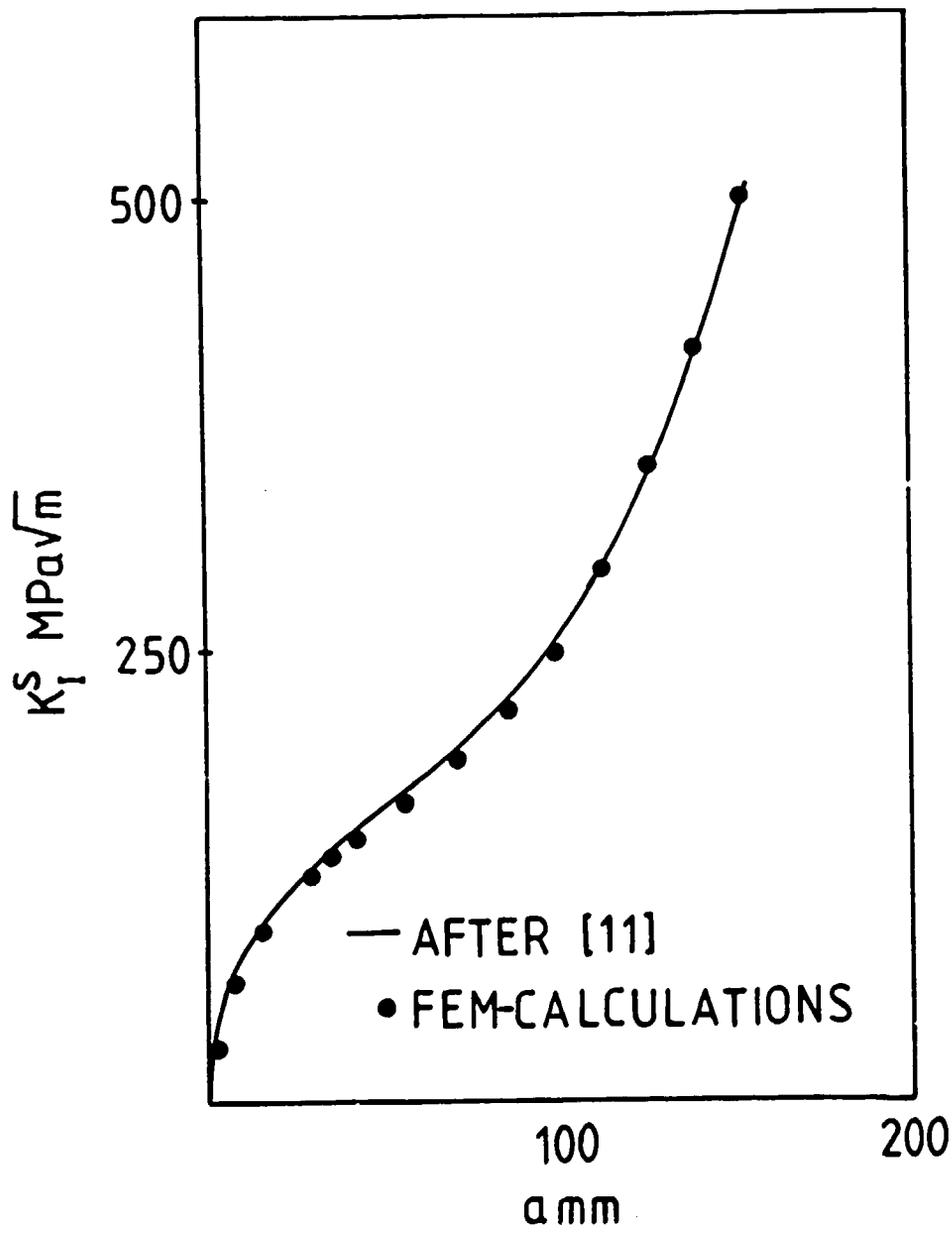

Fig. 6

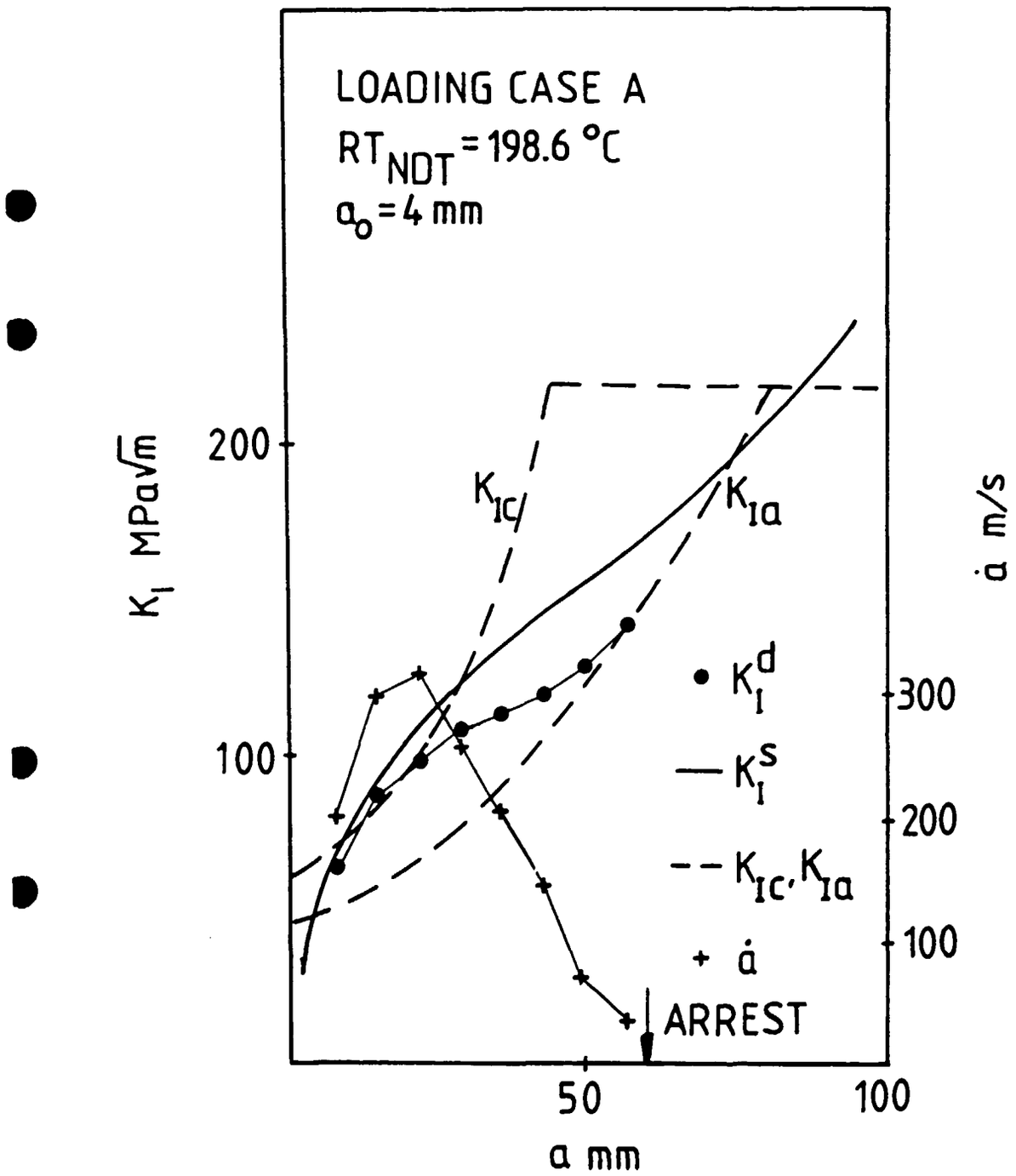
LOADING CASE A
$RT_{NDT}$ = 198.6 °C
$a_o$ = 4 mm
$K_I$ MPa√m
200
100
$K_{Ic}$
$K_{Ia}$
$K_I^d$
$K_I^s$
$K_{Ic}, K_{Ia}$
ȧ
ARREST
50
100
a mm
ȧ m/s
300
200
100

Fig. 7

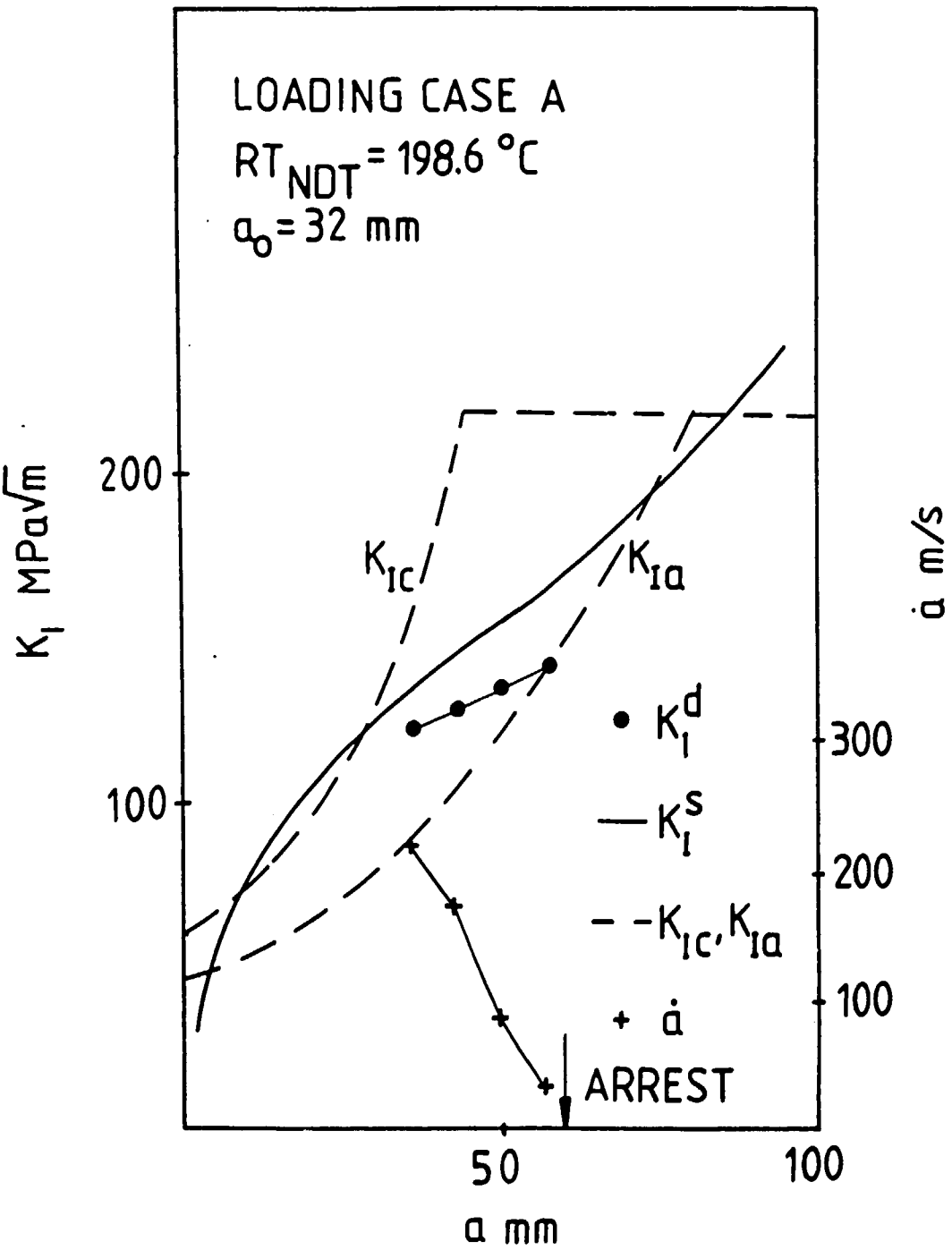
LOADING CASE A
RT_NDT = 198.6 °C
a_o = 32 mm
K_I MPa√m
200
100
K_Ic
K_Ia
• K_I^d
— K_I^s
- - K_Ic, K_Ia
+ ȧ
ARREST
300
200
100
ȧ m/s
50
100
a mm

Fig. 8

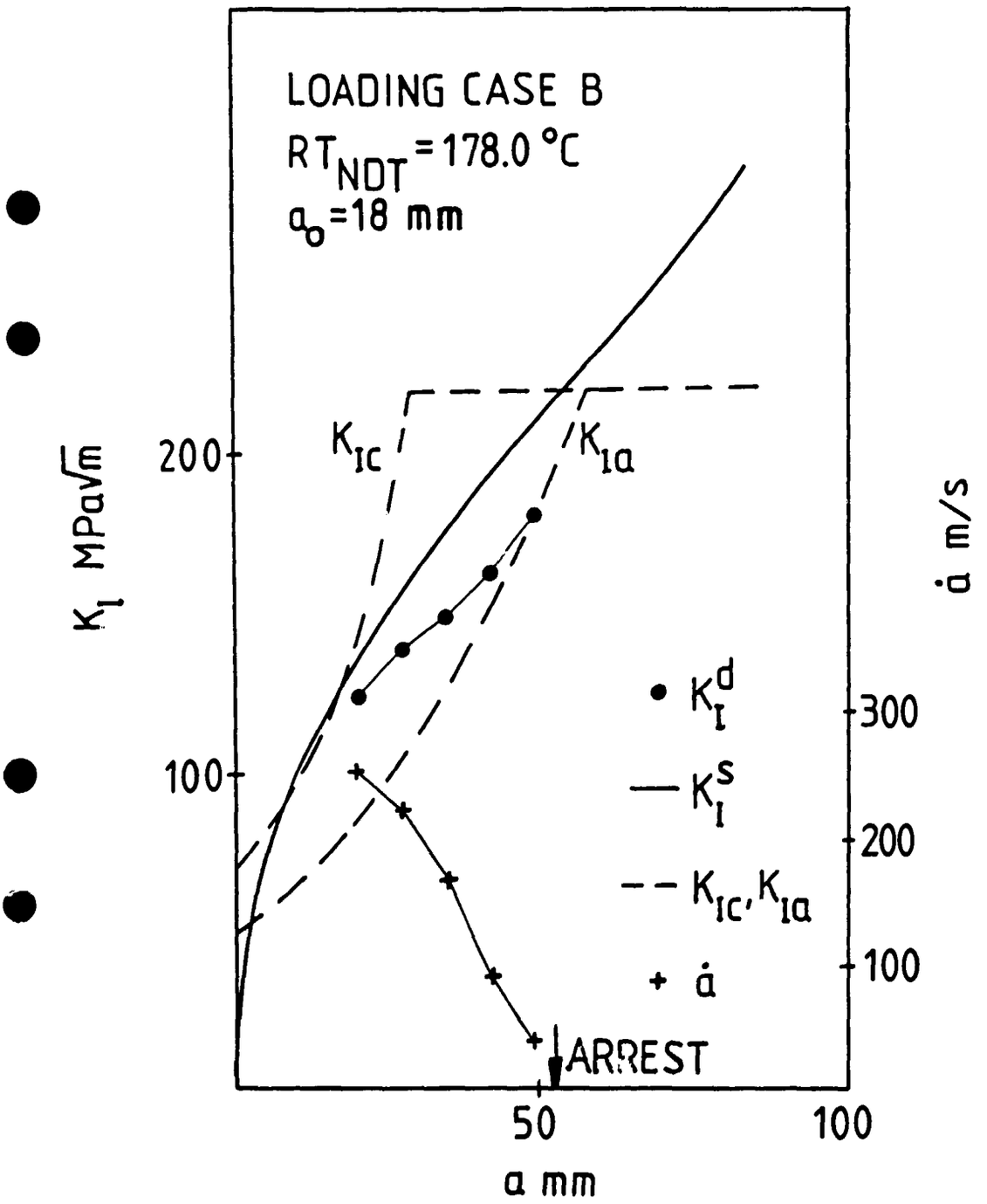
LOADING CASE B
RT$_{NDT}$ = 178.0 °C
$a_o$ = 18 mm
$K_{IC}$
$K_{Ia}$
200
100
$K_I$ MPa$\sqrt{m}$
$K_I^d$
$K_I^s$
$K_{IC}$, $K_{Ia}$
ȧ
ARREST
300
200
100
ȧ m/s
50
100
a mm

Fig. 9

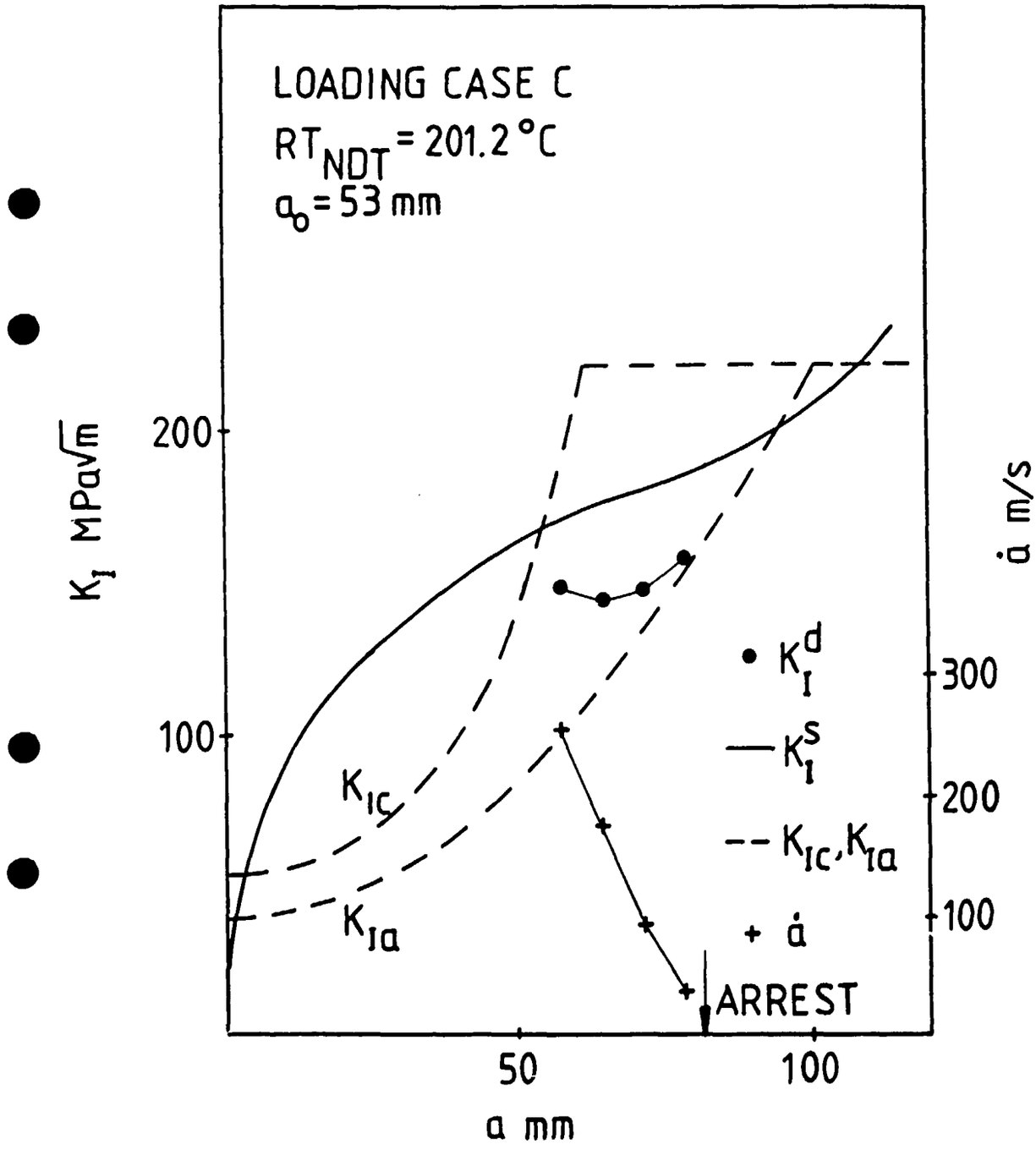
LOADING CASE C
RT$_{NDT}$ = 201.2 °C
$a_o$ = 53 mm
$K_I$ MPa$\sqrt{m}$
200
100
$K_{IC}$
$K_{Ia}$
$K_I^d$
$K_I^s$
$K_{IC}$, $K_{Ia}$
+ ȧ
ARREST
300
200
100
ȧ m/s
50
100
a mm

Fig. 10

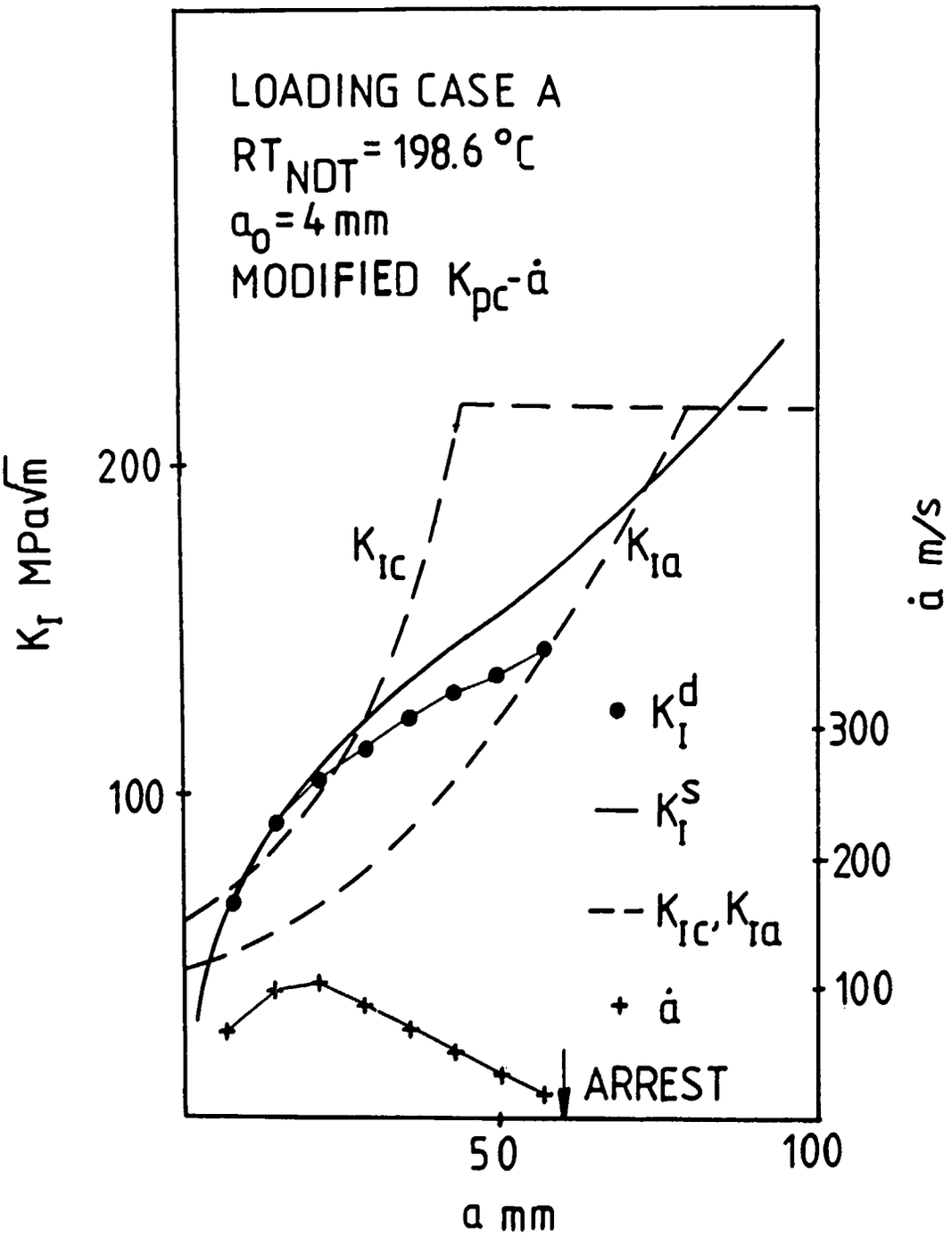
LOADING CASE A
$RT_{NDT}$ = 198.6 °C
$a_0$ = 4 mm
MODIFIED $K_{pc}$-$\dot{a}$
$K_I$ MPa$\sqrt{m}$
200
100
$K_{IC}$
$K_{Ia}$
$\dot{a}$ m/s
300
200
100
$K_I^d$
$K_I^s$
$K_{IC}$, $K_{Ia}$
$\dot{a}$
ARREST
50
100
a mm

Fig. 11

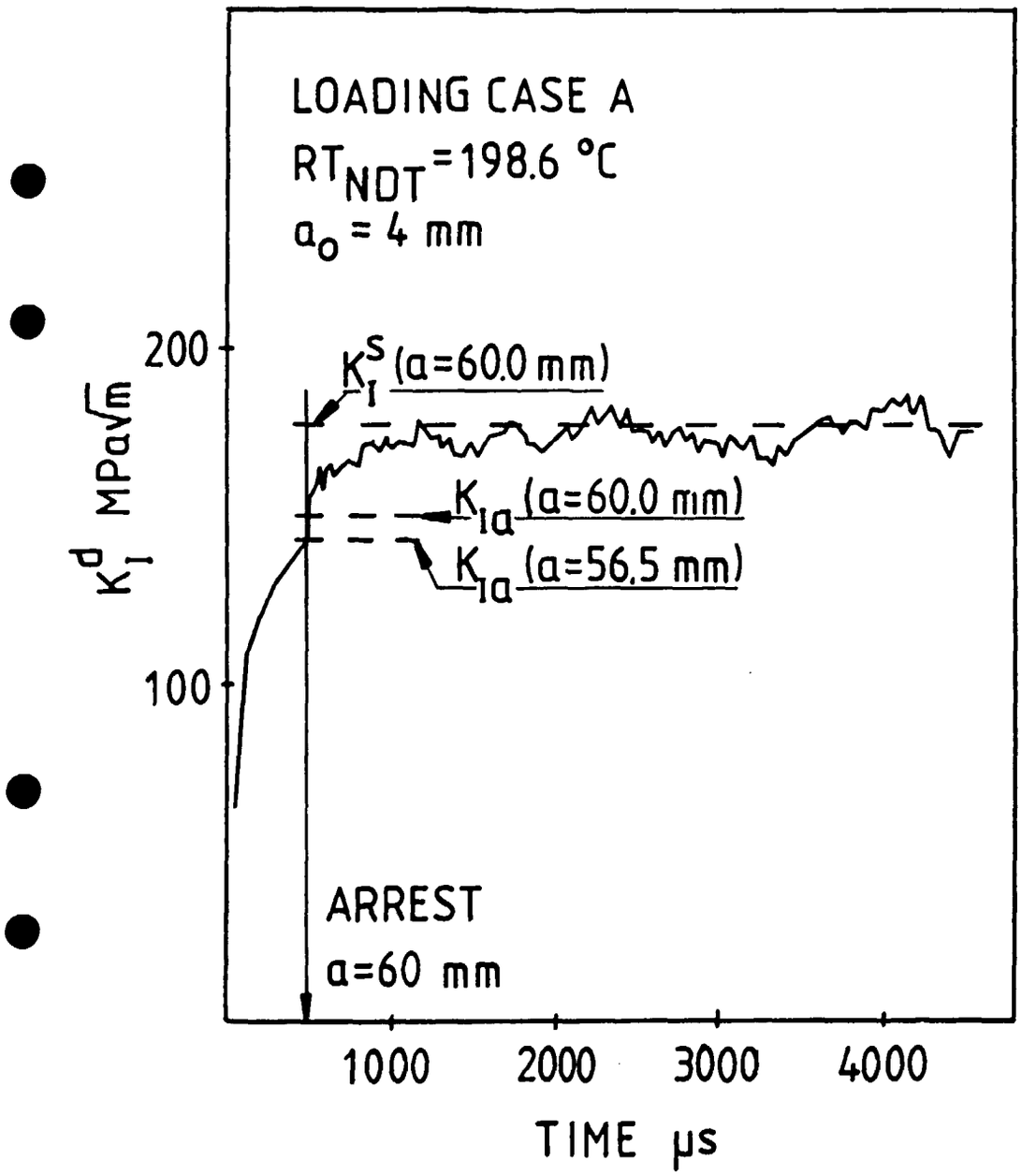
LOADING CASE A
RT_NDT = 198.6 °C
a_o = 4 mm
K_I^S (a=60.0 mm)
K_Ia (a=60.0 mm)
K_Ia (a=56.5 mm)
ARREST
a=60 mm
200
100
K_I^d MPa√m
1000
2000
3000
4000
TIME µs